Interferometric Imaging of Acoustical Phenomena using High-speed Polarization Camera and 4-step Parallel Phase-shifting Technique

K. Ishikawa[1], K. Yatabe[1], Y. Ikeda[1], Y. Oikawa[1],
T. Onuma[2], H. Niwa[2], M. Yoshii[3]
[1]Department of Intermedia Art and Science, Waseda University, 3-4-1 Ohkubo, Shinjuku-ku, Tokyo, 169-8555 JAPAN
[2]Photron limited, 1-105 Kanda-jinbocho, Chiyoda-ku, Tokyo, 101-0051 JAPAN
[3]Kiyohara Optics Inc., 6-23-2 Shinjuku, Shinjuku-ku, Tokyo, 160-0022 JAPAN

ABSTRACT

Imaging of sound aids the understanding of the acoustical phenomena such as propagation, reflection, and diffraction, which is strongly required for various acoustical applications. The imaging of sound is commonly done by using a microphone array, whereas optical methods have recently been interested due to its contactless nature. The optical measurement of sound utilizes the phase modulation of light caused by sound. Since light propagated through a sound field changes its phase as proportional to the sound pressure, optical phase measurement technique can be used for the sound measurement. Several methods including laser Doppler vibrometry and Schlieren method have been proposed for that purpose. However, the sensitivities of the methods become lower as a frequency of sound decreases. In contrast, since the sensitivities of the phase-shifting technique do not depend on the frequencies of sounds, that technique is suitable for the imaging of sounds in the low-frequency range. The principle of imaging of sound using parallel phase-shifting interferometry was reported by the authors (K. Ishikawa *et al.*, Optics Express, 2016). The measurement system consists of a high-speed polarization camera made by Photron Ltd., and a polarization interferometer. This paper reviews the principle briefly and demonstrates the high-speed imaging of acoustical phenomena. The results suggest that the proposed system can be applied to various industrial problems in acoustical engineering.

Keywords: Sound, acousto-optic effect, loudspeaker, quantitative measurement

1. INTRODUCTION

Imaging is a powerful tool for the understanding of physical phenomena. In acoustics, imaging of a sound field, a spatial distribution of sound pressure, aids the comprehension of the acoustical phenomena including propagation, reflection, diffraction and resonance of sound. The understanding of the acoustical phenomena is an essential factor for solving various acoustical problems.

Schlieren method has long been used for the imaging of a sound field.[(1–5)] Since its sensitivity is increased as the frequency of sound increases, the Schlieren method is effective for the imaging of ultrasound. However, it is not easy to use that for low-frequency sound in air due to the decrease of the sensitivity although some recent research success to image audible sound fields in air.[(1–3)] Laser Doppler vibrometer (LDV) is also often used for the imaging.[(6–14)] Although it can detect sound in air, it is hard to apply LDV to a non-stationary field because it requires a scanning process for the imaging. Some other methods have also been proposed[(15–21)]; nevertheless, the quantitative and single-shot imaging of a low-frequency sound field has not been achieved.

The authors reported the imaging of a sound field by using parallel phase-shifting interferometry (PPSI)[(22–25)] and high-speed polarization camera[(26)] in 2016.[(27)] Since the frequency-dependence as Schlieren method and LDV does not exist for the PPSI, the imaging of a low-frequency sound field is achieved by the proposed method. The use of the high-speed polarization camera enables to acquire an instantaneous field. This paper describes the principle briefly and demonstrates the high-speed imaging of acoustical phenomena including propagation, reflection, and diffraction. The experimental results indicate that the imaging of acoustical phenomena is achieved by the proposed method, and that is helpful for the understanding of the phenomena.

2. METHODS

2.1 Acousto-optic effect

The principle of the optical measurement of sound is based on the acousto-optic effect, which is well known as the modulation of light by sound. By assuming adiabatic change and using the Gladstone-Dale relation, the relation between refractive index of air and sound pressure can be approximated by

$$n(\boldsymbol{r},t) = n_0 + \frac{n_0-1}{\gamma p_0} p(\boldsymbol{r},t), \tag{1}$$

where $\boldsymbol{r} \in \mathbb{R}^3$ is the three-dimensional position vector, t is the time, n is the refractive index, n_0 and p_0 are the relative refractive index and pressure under static conditions, p is the sound pressure, and γ is the specific heat ratio. Light propagates through the sound field can be represented by

$$\boldsymbol{E}(\boldsymbol{r},t) = \boldsymbol{E}_0(\boldsymbol{r},t)e^{i(\omega t+\phi(\boldsymbol{r},t))}, \tag{2}$$

where $\boldsymbol{E}_0$ is the complex amplitude vector, ω is the angular frequency of light, and ϕ is the phase term that is given by

$$\phi(\boldsymbol{r},t) = k\int_{L(\boldsymbol{r})} n(\boldsymbol{l},t)d\boldsymbol{l} = kn_0|\boldsymbol{L}| + k\frac{n_0-1}{\gamma p_0}\int_{L(\boldsymbol{r})} p(\boldsymbol{l},t)d\boldsymbol{l}, \tag{3}$$

where k is the wave number of light in vacuum, and $\boldsymbol{L}(\boldsymbol{r})$ is the path of light.[27] In a weak sound field, the path of light, $\boldsymbol{L}$, can be approximated as a line; thus, the phase of light is proportional to the line integration of sound pressure.

2.2 Parallel phase-shifting interferometry

Phase-shifting interferometry is widely used for quantitative measurement of the two-dimensional phase distribution of light.[28] Since it requires phase-shifted multiple images, it is not easy to acquire phase distribution of non-stationary target. Awatsuji *et al.* and Millerd *et al.* proposed PPSI that can obtain multiple phase-shifted images simultaneously.[22–25] By combining the PPSI and high-speed polarization camera[26], high-speed and quantitative imaging of transient phenomena has been achieved[29].

Figure 1 illustrates the schematic of the measurement system consisted of the Fizeau type polarization interferometer[30] and high-speed polarization camera. The contra-rotated circular lights, which are the object and reference lights, are combined and incident into the polarization camera. The phase-shifting array device, which is consist of four types of linear polarizers, is mounted onto the image sensor. Each element of the array device corresponds to each pixel of the image sensor. The intensity of detected light can be written by

$$I(\theta) = \mathrm{A} + \mathrm{B}\cos(\Delta\phi + 2\theta), \tag{4}$$

where θ is the azimuth of the linear polarizer, A is the background illumination, B is the intensity of the interference fringe, and $\Delta\phi$ is the phase difference between the object and reference lights[31]. Since the azimuth of the linear polarizers of the high-speed polarization camera, θ, are $\{0, \pi/4, \pi/2, 3\pi/4\}$, the phase difference, $\Delta\phi$, is obtained by common four-step algorithm;

$$\Delta\phi = \arctan\frac{I(3\pi/4)-I(\pi/4)}{I(0)-I(\pi/2)}, \tag{5}$$

where arctan is the four-quadrant inverse tangent. One phase value is obtained from four pixel values of the camera that is depicted in Fig.1. As described in the previous subsection, the phase of light is modulated by sound. Thus, the obtained phase distribution by Eq. (5) includes the sound information in the object arm. That is the principle of the sound field imaging by PPSI and high-speed polarization camera.

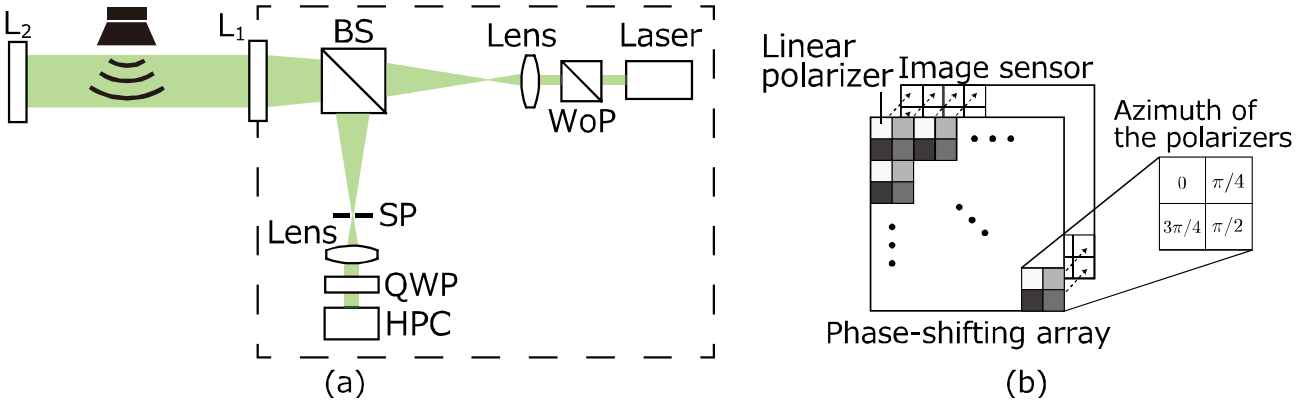

Figure 1: System schematic. (a) The Fizeau type polarization interferometer. The dashed line indicates the case of the interferometer. WoP: Wollaston prism, BS: beam splitter, L1 and L2: lenses to transmit and reflect lights, QWP: quarter wave plate, and HPC: high-speed polarization camera. The sound field between L1 and L2 is measured. (b) The high-speed polarization camera. The phase-shifted array device is mounted on the image sensor. The azimuths of the polarizers are 0, $\pi/4$, $\pi/2$, and $3\pi/4$. The single phase value is calculated from the four phase-shifted intensities.

3. EXPERIMENTS

The experiments were designed to show the availability of the proposed system for the imaging of acoustical phenomena. Metal plates were placed in a measurement area to yield reflection and diffraction of a sound wave. Sound waves were emitted from loudspeakers and the resultant sound fields were measured by the proposed system. The images of the sound fields were realized via the instantaneous phase distribution of detected lights.

3.1 Experimental conditions

Table 1 shows the experimental conditions. The ultrasonic transducer and tweeter were used as sound sources and driven by pure tone of 40,000 Hz and 20,000 Hz, respectively. For the high-speed polarization camera, CRYSTA PI-1P made by Photron Ltd., was used. There is the tradeoff between the frame rate and image size; 7000 fps is the highest frame rate which can use the full image size of the camera. In order to use the full resolution, the frame rate of the camera was 7000 fps. The exposure time was shorter than half periods of the sounds. The laser with a wavelength of 532 nm and power of 70 mW was used. The data calculation scheme was followed:

1. the wrapped phase was calculated by Eq. (5),
2. temporal band pass filters were applied to the wrapped phase at each pixel,
3. averaging of images where the phase of emitted sound wave coincided was conducted.

By applying the band pass filter, slow fluctuation of refractive index caused by vibration, air flow, and thermal sources can be removed, while that by the sound remains. The filters were infinite impulse response band pass filters whose bandwidth was 100 Hz and center frequencies were the frequencies of sounds.

3.2 Results

Figure 2 shows the obtained sound fields when 40,000 Hz and 20,000 Hz sound waves were emitted from the ultrasonic transducer and tweeter, respectively. The transducers were placed on the left side of the image. The length of a side of the square is 100 mm. The circle inside the square is corresponding to the beam cross-section. It can be seen that the sound waves are clearly visualized. The shapes of emitted sound waves differ widely; the sound wave of 40,000 Hz is a nearly spherical wave, while that of 20,000 Hz is an approximately planar wave. It may be due to the difference of structure of the transducers and the wavelength of the sound waves. It is suggested that such imaging results can be used for the design of transducers. Note that, the phase values of obtained images can be converted to the acoustical values by multiplying the coefficients as described in Eq. (3); thus, the quantitative imaging of the acoustical properties can be achieved.[27]

Table 1: Experimental conditions

Transducer	Ultrasonic transducer MURATA MA40S4S	Dome tweeter FOSTEX FT 48D
Sound frequency	40,000 Hz	20,000 Hz
Sound wavelength	8.6 mm	17 mm
Sound waveform	Sinusoidal	Sinusoidal
Frame rate	7000 fps	7000 fps
Exposure time	1/101000 s	1/49000 s
Size of phase image	512 × 512	512 × 512
Distance between adjacent data	0.22 mm	0.22 mm
Number of averaging	100	100

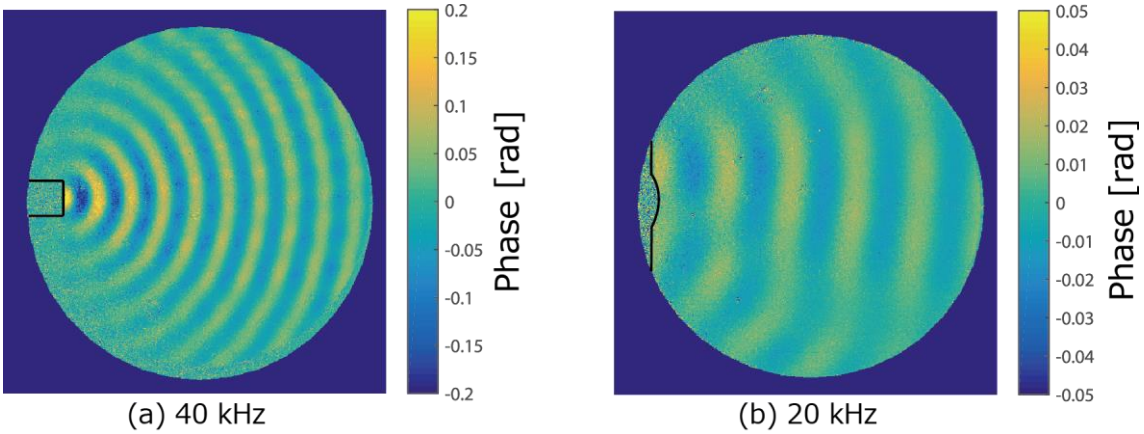

Figure 2: Imaging of sound fields generated by (left) the ultrasonic transducer, and (right) the dome tweeter. The black lines indicate the edge of the transducers.

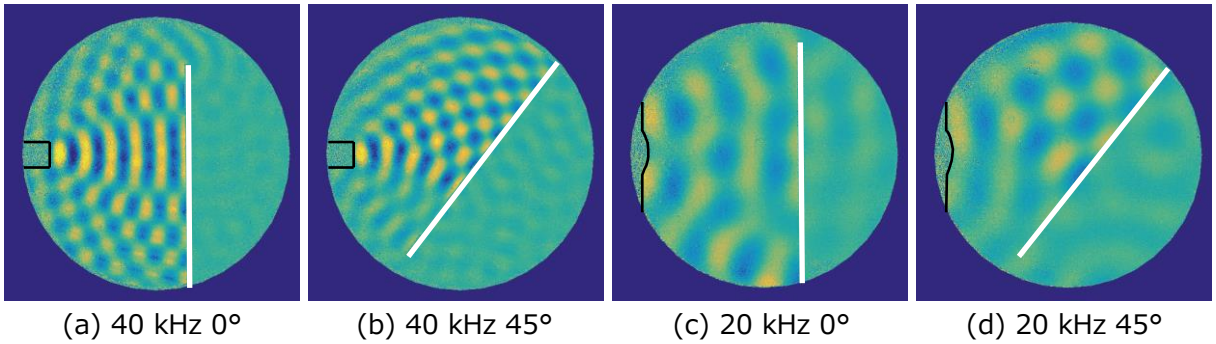

Figure 3: Reflection of sound waves by a thin metal plate. The black lines indicate the edge of the transducers and the white lines indicate the plate.

Figure 3 shows the reflection of the sound waves by a thin metal plate whose thickness is 1 mm. The plate was placed at the center of the images vertically and diagonally. The patterns of the phase are appeared by the superposition of the incident wave and reflected wave. In Fig. 3(a), the complicated pattern appears because of the spherical shape of the sound wave. In contrast, the sound field in Fig. 3(c) does not differ widely from Fig. 2(b). It should be because incident wave and reflected wave are added in almost same phase due to the planar shape of the wave. For the diagonal cases, the lattice patterns can be seen in both 40,000 Hz and 20,000 Hz sound waves. The time-sequential images of Fig. 3(a) are shown in Fig. 4. The seven images shown in the figure are corresponding to one period of the sound field. The interference pattern changes as the phase of incident sound wave changes.

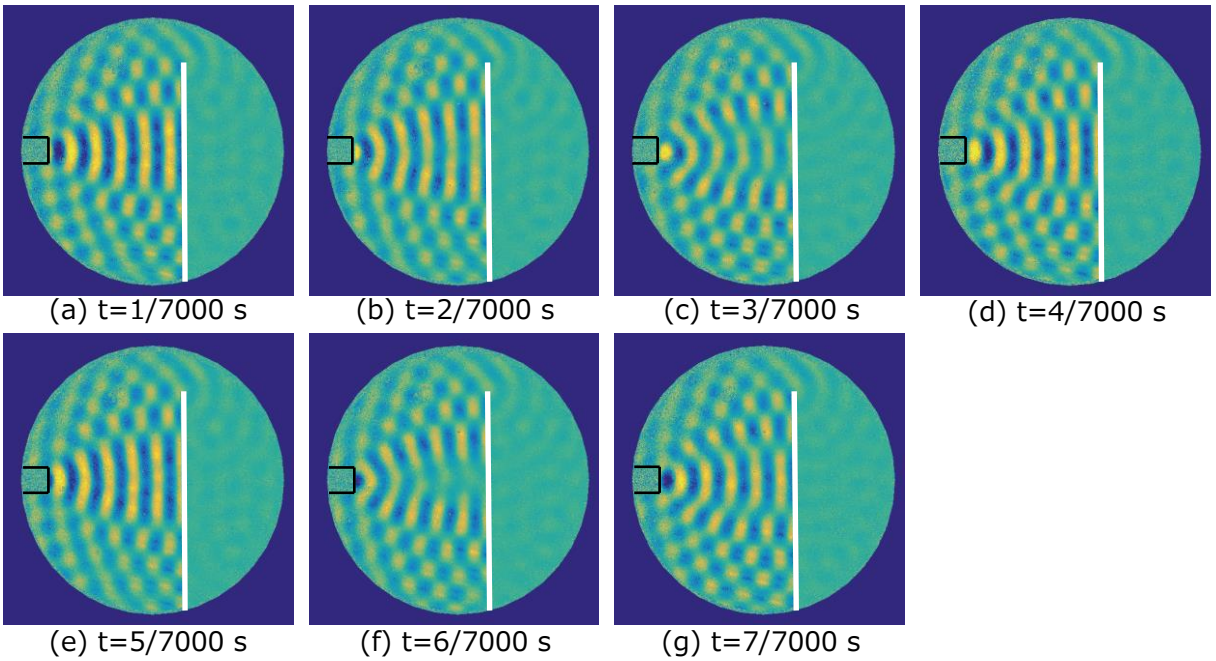

Figure 4: Temporal variation of the sound field due to the reflection of 40 kHz sound wave by a thin metal plate. The time interval is 1/7000 s.

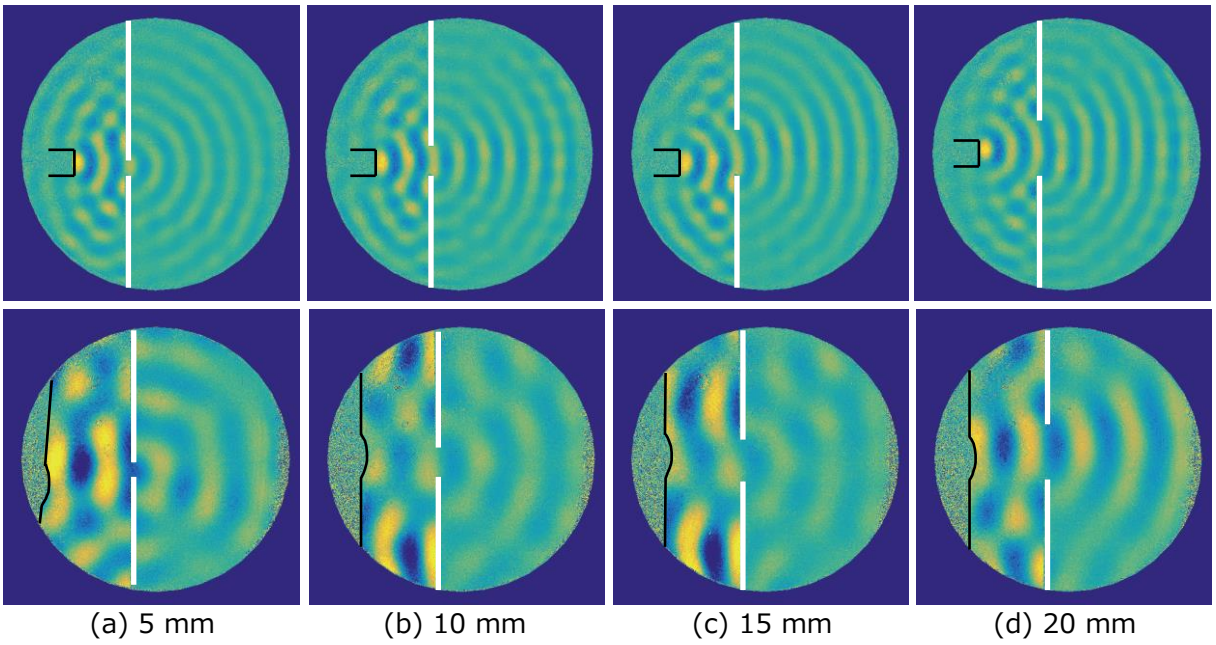

Figure 5: Diffraction of sound waves by a single slit (top: 40,000 Hz, bottom: 20,000 Hz). The slit width is 5 mm, 10 mm, 15 mm, and 20 mm.

Figure 5 shows the diffraction of sound waves by a single slit. The slit was made by two thin metal plates. When the slit width is 5 mm and frequency of sound is 40,000 Hz, the diffracted wave is almost spherical. As slit width increases, the wavefront becomes more planar. At the left of the slit in sound fields of 20,000 Hz, the resonances occurred between the metal plates and the baffle of the dome tweeter.

4. CONCLUSIONS

This paper presented the imaging of acoustical phenomena using the PPSI and high-speed polarization camera. High-speed imaging (frame rate was 7000 fps, and exposure time was half of the period of generated sound waves) of the sound fields was achieved. Propagation, reflection, and diffraction of 40,000 Hz and 20,000 Hz sound waves were clearly visualized. The obtained images provide the information of the sound fields including characteristics of transducers and objects. Since such high spatial resolution imaging of a sound field is difficult to achieve by using a conventional technique such as microphone array, this method should produce new experimental knowledge about the various acoustical phenomena. Future work should apply the proposed method to actual acoustical problems. Furthermore, recently developed signal processing methods[32–35] should be applied to the proposed method for improving the measurement results.

ACKNOWLEDGMENT

This work was supported in part by Japan Society for the Promotion of Science (JSPS) Grants-in-Aid for JSPS Fellows (16J06772, 15J08043).

REFERENCES

[1] Bucaro, J. A. and Dardy, H. D., "Visualization of ultrasonic waves in air, " *J. Acoust. Soc. Am.*, 62(6), 1506-1507 (1977).

[2] Krehl, P. and Engemann, S., "August Toepler - The first who visualized shock waves, " *Shock Waves*, 5(1-2), 1-18 (1995).

[3] Hargather, M. J., Settles, G. S., and Madalis, M. J., "Schlieren imaging of loud sounds and weak shock waves in air near the limit of visibility, " *Shock Waves*, 20(1), 9-17 (2010).

[4] Chitanont, N., Yaginuma, K., Yatabe, K., and Oikawa, Y., "Visualization of sound field by means of Schlieren method with spatio-temporal filtering," *Proc. IEEE ICASSP 2015*, 3, 509-513 (2015).

[5] Chitanont, N., Yatabe, K., Ishikawa, K., and Oikawa, Y., "Spatio-temporal filter bank for visualizing audible sound field by Schlieren method, " *Appl. Acoust.*, 115, 109-120 (2017).

[6] Nakamura, K., Hirayama, M., and Ueha, S., "Measurements of air-borne ultrasound by detecting the modulation in optical refractive index of air, " *Proc. IEEE Ultrason. Symp. 2002.*, 1(c), 609-612 (2002).

[7] Harland, A. R., Petzing, J. N., and Tyrer, J. R., "Non-Invasive measurements of underwater pressure fields using laser Doppler velocimetry, " *J. Sound Vib.*, 252(1), 169-177 (2002).

[8] Zipser, L., Franke, H., Olsson, E., Molin, N.-E., and Sjödahl, M., "Reconstructing two-dimensional acoustic object fields by use of digital phase conjugation of scanning laser vibrometry recordings, " *Appl. Opt.*, 42(29), 5831-5838 (2003).

[9] Zipser, L. and Franke, H., "Laser-scanning vibrometry for ultrasonic transducer development, " *Sens. Actuators A Phys.*, 110(1–3), 264-268 (2004).

[10] Oikawa, Y., Ikeda, Y., Goto, M., Takizawa, T., and Yamasaki, Y., "Sound field measurements based on reconstruction from laser projections, " *Proc. IEEE ICASSP 2005*, 4, 661-664 (2005).

[11] Torras-Rosell, A., Barrera-Figueroa, S., and Jacobsen, F., "Sound field reconstruction using acousto-optic tomography, " *J. Acoust. Soc. Am.*, 131(5), 3786-3793 (2012).

[12] Yatabe, K. and Oikawa, Y., "PDE-based interpolation method for optically visualized sound field, " *Proc. IEEE ICASSP 2014*, 5, 4738-4742 (2014).

[13] Yatabe, K. and Oikawa, Y., "Optically visualized sound field reconstruction based on sparse selection of point sound sources, " *Proc. IEEE ICASSP 2015*, 504-508 (2015).

[14] Ikeda, Y., Okamoto, N., Konishi, T., Oikawa, Y., Tokita, Y., and Yamasaki, Y., "Observation of traveling wave with laser tomography, " *Acoust. Sci. Technol.*, 37(5), 231-238 (2016). [The original paper (in Japanese) is published in the *J. Acoust. Soc. Jpn.*, 64(3), 142-149 (2008).]

[15] Sakoda, T. and Sonoda, Y., "Visualization of sound field with uniform phase distribution using laser beam microphone coupled with computerized tomography method, " *Acoust. Sci. Technol.*, 29(4), 295-299 (2008).

[16] Sonoda, Y. and Nakazono, Y., "Development of optophone with no diaphragm and application to sound measurement in jet flow, " *Adv. Acoust. Vib.*, 2012, 1-17 (2012).

[17] Bertling, K., Perchoux, J., Taimre, T., Malkin, R., Robert, D., Rakić, A. D., and Bosch, T., "Imaging of acoustic fields using optical feedback interferometry, " *Opt. Express*, 22(24), 30346-30356 (2014).

[18] Løkberg, O. J., "Sound in flight: measurement of sound fields by use of TV holography, " *Appl. Opt.*, 33(13), 2574-2584 (1994).

[19] Løkberg, O. J., "Recording of sound emission and propagation in air using TV holography, " *J. Acoust. Soc. Am.*, 96(4), 2244-2250 (1994).
[20] Mizutani, K., Ezure, T., Nagai, K., and Yoshioka, M., "Measurement of sound fields information using Mach-Zehnder interferometer, " *Jpn. J. Appl. Phys.*, 40(Part 1, No. 5B), 3617-3620 (2001).
[21] Matoba, O., Inokuchi, H., Nitta, K., and Awatsuji, Y., "Optical voice recorder by off-axis digital holography, " *Opt. Lett.*, 39(22), 6549-6552 (2014).
[22] Awatsuji, Y., Sasada, M., and Kubota, T., "Parallel quasi-phase-shifting digital holography, " *Appl. Phys. Lett.*, 85(6), 1069-1071 (2004).
[23] Awatsuji, Y., "Parallel Phase-Shifting Digital Holography," in [Multi-Dimensional Imaging], John Wiley & Sons, Ltd, Chichester, UK, 1-23 (2014).
[24] Millerd, J., Brock, N., Hayes, J., North-Morris, M., Kimbrough, B., and Wyant, J., "Pixelated Phase-Mask Dynamic Interferometers, " *Proc. Fringe 2005*, 640-647 (2005).
[25] Novak, M., Millerd, J., Brock, N., North-Morris, M., Hayes, J., and Wyant, J., "Analysis of a micropolarizer array-based simultaneous phase-shifting interferometer, " *Appl. Opt.*, 44(32), 6861-6868 (2005).
[26] Onuma, T. and Otani, Y., "A development of two-dimensional birefringence distribution measurement system with a sampling rate of 1.3 MHz, " *Opt. Commun.*, 315, 69-73 (2014).
[27] Ishikawa, K., Yatabe, K., Chitanont, N., Ikeda, Y., Oikawa, Y., Onuma, T., Niwa, H., and Yoshii, M., "High-speed imaging of sound using parallel phase-shifting interferometry, " *Opt. Express*, 24(12), 12922-12932 (2016).
[28] Schreiber, H. and Bruning, J. H., "Phase Shifting Interferometry, " in [Optical Shop Testing], Third Ed., John Wiley & Sons, Inc., Hoboken, NJ, USA, 547-666 (2006).
[29] Kakue, T., Yonesaka, R., Tahara, T., Awatsuji, Y., Nishio, K., Ura, S., Kubota, T., and Matoba, O., "High-speed phase imaging by parallel phase-shifting digital holography, " *Opt. Lett.*, 36(21), 4131-4133 (2011).
[30] Yatagai, T., Jackin, B., Ono, A., Kiyohara, K., Noguchi, M., Yoshii, M., Kiyohara, M., Niwa, H., Ikuo, K., and Onuma, T., "Instantaneous phase-shifting Fizeau interferometry with high-speed pixelated phase-mask camera, " *Proc. SPIE 9660*, 966018 (2015).
[31] Okoomian, H. J., "A two-beam polarization technique to measure optical phase, " *Appl. Opt.*, 8(11), 2363-2365 (1969).
[32] Yatabe, K., Ishikawa, K., and Oikawa, Y., "Improving principal component analysis based phase extraction method for phase-shifting interferometry by integrating spatial information, " *Opt. Express*, 24(20), 22881-22891 (2016).
[33] Yatabe, K. and Oikawa, Y., "Convex optimization-based windowed Fourier filtering with multiple windows for wrapped-phase denoising, " *Appl. Opt.*, 55(17), 4632-4641 (2016).
[34] Yatabe, K., Ishikawa, K., and Oikawa, Y., "Compensation of fringe distortion for phase-shifting three-dimensional shape measurement by inverse map estimation, " *Appl. Opt.*, 55(22), 6017-6024 (2016).
[35] Yatabe, K., Ishikawa, K., and Oikawa, Y., "Simple, flexible and accurate phase retrieval method for generalized phase-shifting interferometry, " *J. Opt. Soc. Am. A*, 34(1), 87-96 (2017).